

# Contactium: A strongly correlated model system

Jerzy Cioslowski,<sup>1, a)</sup> Berthold-Georg Englert,<sup>2, 3, 4</sup> Martin-Isbjörn Trappe,<sup>2</sup> and Jun Hao Hue<sup>2</sup>

<sup>1)</sup>*Institute of Physics, University of Szczecin, Wielkopolska 15, 70-451 Szczecin, Poland*

<sup>2)</sup>*Centre for Quantum Technologies, National University of Singapore, 3 Science Drive 2, Singapore 117543, Singapore*

<sup>3)</sup>*Department of Physics, National University of Singapore, 2 Science Drive 3, Singapore 117542, Singapore*

<sup>4)</sup>*MajuLab, CNRS-UCA-SU-NUS-NTU International Joint Research Unit, Singapore*

(Posted on the arXiv on 27 March 2023)

At the limit of an infinite confinement strength  $\omega$ , the ground state of a system that comprises two fermions or bosons in a harmonic confinement interacting through the Fermi–Huang pseudopotential remains strongly correlated. A detailed analysis of the one-particle description of this “contactium” reveals several peculiarities that are not encountered in conventional model systems (such as the two-electron harmonium atom, ballium, and spherium) involving Coulombic interparticle interactions. First of all, none of the natural orbitals (NOs)  $\{\psi_n(\omega; \mathbf{r})\}$  of the contactium is unoccupied, which implies nonzero collective occupancies for all the angular momenta. Second, the NOs and their nonascendingly ordered occupation numbers  $\{\nu_n\}$  turn out to be related to the eigenfunctions and eigenvalues of a zero-energy Schrödinger equation with an attractive Gaussian potential. This observation enables the derivation of their properties such as the  $n^{-4/3}$  asymptotic decay of  $\nu_n$  at the  $n \rightarrow \infty$  limit (which differs from that of  $n^{-8/3}$  in the Coulombic systems), the independence of the confinement energy  $v_n = \langle \psi_n(\omega; \mathbf{r}) | \frac{1}{2}\omega^2 r^2 | \psi_n(\omega; \mathbf{r}) \rangle$  of  $n$ , and the  $n^{-2/3}$  asymptotic decay of the respective contribution  $\nu_n t_n$  to the kinetic energy. Upon suitable scaling, the weakly occupied NOs of the contactium turn out to be virtually identical with those of the two-electron harmonium atom at the  $\omega \rightarrow \infty$  limit, despite the entirely different interparticle interactions in these systems.

## I. INTRODUCTION

Interactions between particles confined by external potentials introduce correlations that limit the accuracy of simple descriptions (such as the Hartree–Fock and Gross–Pitaevskii approximations for fermions and bosons, respectively) of their quantum states. This limitation is lifted upon employment of more sophisticated formalisms based upon quantities such as the one-particle density matrix (the 1-matrix), the one-particle density, and various one-particle functions (commonly called orbitals). In fact, in the case of Coulombic systems (i.e. atoms, ions, and molecules), formalisms that involve these quantities are the mainstay of approaches to the electron correlation problem.<sup>1</sup> Development and implementation of these approaches is greatly aided by benchmarking on model systems for which exact wave functions can be written in closed forms.

One of such systems is the harmonium atom (also known as hookium or Hooke’s atom) that comprises Coulombically interacting fermions in a harmonic external potential. Its two-particle version,<sup>2–5</sup> introduced over sixty years ago,<sup>6</sup> has been extensively used (especially with the confinement strengths that correspond to compact wave functions) in conjunction with diverse formalisms of quantum chemistry.<sup>7,8</sup> Other model systems, such as spherium (i.e. two electrons restricted to the surface of a sphere<sup>9</sup>) and ballium (i.e. two electrons trapped in a

spherical box<sup>10</sup>) have also been considered but found only limited applications due to the fact that, unlike harmonium (which describes three-dimensional quantum dots), they do not pertain to any experimentally realizable physical system.

The 1-matrix functional theory (1-RDMFT) is an emergent approach to the accurate treatment of correlations in species composed of either fermions<sup>11</sup> or bosons<sup>12</sup> that holds a promise of becoming an alternative to density-functional theory (DFT). When formulated in terms of natural orbitals (NOs)  $\{\phi_i(\mathbf{r})\}$ , 1-RDMFT leads to (in principle exact, in practice approximate) functionals for the correlated component of the interparticle interaction energy that are “superuniversal,” i.e. it can be expressed solely in terms of the occupation numbers of the NOs, some spin-related quantities, and the two-particle matrix elements of the interaction potential, such as the two-electron integrals  $\{\langle ij|kl \rangle\} \equiv \{\langle \phi_i(\mathbf{r}_1)\phi_j(\mathbf{r}_2) | |\mathbf{r}_1 - \mathbf{r}_2|^{-1} | \phi_k(\mathbf{r}_1)\phi_l(\mathbf{r}_2) \rangle\}$ .<sup>13</sup> In light of this property, one is tempted to apply this formalism to systems involving the so-called contact (or zero-range) interactions by simply replacing  $|\mathbf{r}_1 - \mathbf{r}_2|^{-1}$  with  $\delta(\mathbf{r}_1 - \mathbf{r}_2)$ , where  $\delta(\mathbf{r})$  is the three-dimensional Dirac delta function. Unfortunately, this simple replacement is not valid due to complications inherent in the underlying Hamiltonian.

The lack of the self-adjointness of Hamiltonians with potential energy terms proportional to  $\delta(\mathbf{r})$  was first recognized by Fermi<sup>14</sup> and then further elaborated by Huang and Yang<sup>15</sup> who concluded that a regularization of  $\delta(\mathbf{r})$  is needed. The resulting Fermi–Huang pseudopotential is now widely used in the description of ultracold atomic and molecular systems in traps.<sup>16</sup>

<sup>a)</sup>To whom all the correspondence should be addressed, e-mail: jerzy@wmf.univ.szczecin.pl

The expressions for the ground-state and excited-state wave functions of a system of two particles (either fermions or bosons) whose potential energy comprises contributions from a harmonic confinement and a term proportional to the Fermi–Huang pseudopotential are known in closed forms.<sup>17</sup> Interestingly, the kinetic and interparticle interaction energy components pertaining to these wave functions are infinite and thus cannot be considered separately. This observation prompts the question whether standard approaches (such as DFT and 1-RDMFT) based upon one-particle quantities are applicable to this new type of a model system for which, in analogy to its Coulombic counterparts (i.e. harmonium, spherium, and ballium), the name “contactium” is coined here.

In this paper, the one-particle description of the contactium is investigated and its peculiarities are uncovered. Although two parameters (i.e. the confinement strength  $\omega$  and the coupling constant  $\beta$  that multiplies the regularized Dirac delta in the Fermi-Huang pseudopotential) control the properties of this system, a simple scaling eliminates one of them. In order to facilitate a direct comparison with the properties of the two-electron harmonium atom,  $\omega$  is varied while  $\beta$  is set to one (which corresponds to a positive-valued scattering length<sup>17</sup>). The main focus of the present study is the  $\omega \rightarrow \infty$  limit at which the contactium remains strongly correlated.

## II. THEORY

The normalized spatial component

$$\begin{aligned} \Psi(\omega; \mathbf{r}_1, \mathbf{r}_2) &= \frac{\omega^{5/4} \Gamma(-\nu)}{2^{3/4} \pi^{9/4} [\psi(-\nu) - \psi(-\nu - \frac{1}{2})]^{1/2}} \\ &\times \exp\left(-\frac{1}{2} \omega (r_1^2 + r_2^2)\right) \\ &\times \frac{U\left(-\nu - \frac{1}{2}, \frac{1}{2}, \frac{1}{2} \omega r_{12}^2\right)}{r_{12}} \end{aligned} \quad (1)$$

of the ground-state wave function of the system under study is an eigenfunction of the nonrelativistic Hamiltonian

$$H = -\frac{1}{2}(\nabla_1^2 + \nabla_2^2) + \frac{1}{2}\omega^2(r_1^2 + r_2^2) + \delta_{\text{reg}}(\mathbf{r}_{12}) \quad (2)$$

that involves the Fermi–Huang pseudopotential  $\delta_{\text{reg}}(\mathbf{r}) = \delta(\mathbf{r}) \frac{r}{|\mathbf{r}|} \cdot \nabla |\mathbf{r}|$ .<sup>14,15,17</sup> Here and in the following,  $\omega$  is the confinement strength,  $\mathbf{r}_{12} = \mathbf{r}_1 - \mathbf{r}_2$ ,  $r_1 = |\mathbf{r}_1|$ ,  $r_2 = |\mathbf{r}_2|$ ,  $r_{12} = |\mathbf{r}_1 - \mathbf{r}_2|$ ,  $\Gamma(t)$  and  $\psi(t) = [\ln \Gamma(t)]'$  are the gamma and digamma functions, respectively,  $U(a, b, t)$  is the Tricomi confluent hypergeometric function, and  $\nu \equiv \nu(\omega)$  is the negative-valued solution of the equation

$$\frac{\Gamma(-\nu - \frac{1}{2})}{\Gamma(-\nu)} = \frac{\omega^{1/2}}{2^{3/2} \pi}. \quad (3)$$

The energy  $E(\omega)$  corresponding to  $\Psi(\omega; \mathbf{r}_1, \mathbf{r}_2)$  equals  $(3 + 2\nu)\omega$ .

Since

$$\begin{aligned} U\left(-\nu - \frac{1}{2}, \frac{1}{2}, \frac{1}{2} \omega r_{12}^2\right) &= \frac{\pi^{1/2}}{\Gamma(-\nu)} - \frac{(2\pi)^{1/2}}{\Gamma(-\nu - \frac{1}{2})} \omega^{1/2} r_{12} + \dots \end{aligned} \quad (4)$$

as  $r_{12} \rightarrow 0$ , Eq. (1) reveals the leading singularity in  $\Psi(\omega; \mathbf{r}_1, \mathbf{r}_2)$  at  $\mathbf{r}_1 \rightarrow \mathbf{r}_2$ . This singularity persists as  $\omega \rightarrow \infty$ , where  $\nu \rightarrow -\frac{1}{2}$ ,  $E(\omega) \rightarrow 2\omega$ , and

$$\begin{aligned} \Psi(\omega; \mathbf{r}_1, \mathbf{r}_2) &\rightarrow \Psi_\infty(\omega; \mathbf{r}_1, \mathbf{r}_2) \\ &= \frac{\omega}{\pi^{3/2}} \exp\left(-\frac{1}{2} \omega (r_1^2 + r_2^2)\right) \left(\frac{1}{r_{12}} - 4\pi\right). \end{aligned} \quad (5)$$

The leading term  $\Psi_\infty(\omega; \mathbf{r}_1, \mathbf{r}_2)$  of the asymptotics (5) is employed in the following considerations.

### A. The natural orbitals and their occupation numbers

Since  $\Psi_\infty(\omega; \mathbf{r}_1, \mathbf{r}_2)$  is totally symmetric, the square-normalized natural orbitals (NOs)  $\{\psi_{nlm}(\omega; \mathbf{r})\}$ , which are eigenfunctions of the homogeneous Fredholm equation of the second kind<sup>18</sup>

$$\int \Psi_\infty(\omega; \mathbf{r}_1, \mathbf{r}_2) \psi_{nlm}(\omega; \mathbf{r}_2) d^3 \mathbf{r}_2 = \lambda_{nl} \psi_{nlm}(\omega; \mathbf{r}_1), \quad (6)$$

are given by products of real-valued, square-normalized radial components  $\{\phi_{nl}(\omega; r)\}$  and angular factors that are real-valued combinations of the respective spherical harmonics  $Y_l^{-m}(\theta, \varphi)$  and  $Y_l^m(\theta, \varphi)$ . The corresponding  $m$ -independent eigenvalues  $\{\lambda_{nl}\}$ , which are indexed in a nonascending order by  $n = 1, 2, \dots$ , are the real-valued natural amplitudes (NAs). Since  $\nabla_1^2 \frac{1}{|\mathbf{r}_1 - \mathbf{r}_2|} = -4\pi \delta(\mathbf{r}_1 - \mathbf{r}_2)$ , combining Eqs. (5) and (6) produces

$$\begin{aligned} \left(-\frac{1}{2} \nabla^2 - \frac{2\omega}{\pi^{1/2} \lambda_{nl}} \exp(-\omega r^2)\right) \\ \times \left[\exp\left(\frac{1}{2} \omega r^2\right) \psi_{nlm}(\omega; \mathbf{r})\right] = 0, \end{aligned} \quad (7)$$

a zero-energy Schrödinger equation in which  $\exp(\frac{1}{2} \omega r^2) \psi_{nlm}(\omega; \mathbf{r})$  and  $-\pi^{-1/2} (2\omega/\lambda_{nl}) \exp(-\omega r^2)$  play the roles of the wave function and the attractive potential, respectively.

The number  $N_l(\kappa)$  of the  $l$ -wave bound states of the spherically symmetric Hamiltonian  $-\frac{1}{2} \nabla^2 - \kappa V(r)$ , where  $V(r) \geq 0$  for all  $r$ , is known to conform to the asymptotic identity<sup>19</sup>

$$\lim_{\kappa \rightarrow \infty} \kappa^{-1/2} N_l(\kappa) = \frac{2^{1/2}}{\pi} \int_0^\infty V(r)^{1/2} dr. \quad (8)$$

Application of this identity to the present case leads to the conclusion that, for a given  $l$  and  $m$ , the large- $n$

asymptotic estimates  $\{\tilde{\lambda}_{nl}\}$  of the NAs read

$$\tilde{\lambda}_{nl} = \frac{2}{\pi^{3/2}} n^{-2}. \quad (9)$$

Similarly, the identity<sup>20</sup>

$$\lim_{\kappa \rightarrow \infty} \kappa^{-3/2} N(\kappa) = \frac{2^{1/2}}{3\pi^2} \int V(\mathbf{r})^{3/2} d^3\mathbf{r} \quad (10)$$

for the number  $N(\kappa)$  of bound states of the Hamiltonian  $-\frac{1}{2}\nabla^2 - \kappa V(\mathbf{r})$ , where  $V(\mathbf{r}) \geq 0$  for all  $\mathbf{r}$ , produces the

There are several equivalent expressions for the NAs. First of all, Eq. (6) readily yields  $\lambda_{nl} = \langle \psi_{nlm}(\omega; \mathbf{r}_1) | \Psi_\infty(\omega; \mathbf{r}_1, \mathbf{r}_2) | \psi_{nlm}(\omega; \mathbf{r}_2) \rangle$ . Second, Eq. (7) implies

$$\lambda_{nl} = \frac{2\omega}{\pi^{1/2}} \frac{\langle \psi_{nlm}(\omega; \mathbf{r}) | \exp(-\omega r^2) | \psi_{nlm}(\omega; \mathbf{r}) \rangle}{\langle \psi_{nlm}(\omega; \mathbf{r}) | \exp(-\frac{1}{2}\omega r^2) T \exp(\frac{1}{2}\omega r^2) | \psi_{nlm}(\omega; \mathbf{r}) \rangle} = \frac{2\omega}{\pi^{1/2}} \frac{u_{nl}}{t_{nl} - v_{nl}}, \quad (12)$$

where  $T$  is the kinetic energy operator and the  $m$ -independent expectation values read, respectively,  $u_{nl} = \langle \psi_{nlm}(\omega; \mathbf{r}) | \exp(-\omega r^2) | \psi_{nlm}(\omega; \mathbf{r}) \rangle$ ,  $t_{nl} = \langle \psi_{nlm}(\omega; \mathbf{r}) | T | \psi_{nlm}(\omega; \mathbf{r}) \rangle$ , and  $v_{nl} = \langle \psi_{nlm}(\omega; \mathbf{r}) | \frac{1}{2}\omega^2 r^2 | \psi_{nlm}(\omega; \mathbf{r}) \rangle$ . Third, since

$$\begin{aligned} 2\omega \lambda_{nl} &= 2\omega \langle \psi_{nlm}(\omega; \mathbf{r}_1) \psi_{nlm}(\omega; \mathbf{r}_2) | \sum_{\mathbf{n}=1}^{\infty} \lambda_{\mathbf{n}} \psi_{\mathbf{n}}(\omega; \mathbf{r}_1) \psi_{\mathbf{n}}(\omega; \mathbf{r}_2) \rangle \\ &= 2\omega \langle \psi_{nlm}(\omega; \mathbf{r}_1) \psi_{nlm}(\omega; \mathbf{r}_2) | \Psi_\infty(\omega; \mathbf{r}_1, \mathbf{r}_2) \rangle = \langle \psi_{nlm}(\omega; \mathbf{r}_1) \psi_{nlm}(\omega; \mathbf{r}_2) | H | \Psi_\infty(\omega; \mathbf{r}_1, \mathbf{r}_2) \rangle \\ &= \langle \psi_{nlm}(\omega; \mathbf{r}_1) \psi_{nlm}(\omega; \mathbf{r}_2) | H | \sum_{\mathbf{n}=1}^{\infty} \lambda_{\mathbf{n}} \psi_{\mathbf{n}}(\omega; \mathbf{r}_1) \psi_{\mathbf{n}}(\omega; \mathbf{r}_2) \rangle \\ &= 2\lambda_{nl}(t_{nl} + v_{nl}) + \langle \psi_{nlm}(\omega; \mathbf{r}_1) \psi_{nlm}(\omega; \mathbf{r}_2) | \delta_{\text{reg}}(\mathbf{r}_{12}) | \Psi_\infty(\omega; \mathbf{r}_1, \mathbf{r}_2) \rangle \\ &= 2\lambda_{nl}(t_{nl} + v_{nl}) - \frac{4\omega}{\pi^{1/2}} u_{nl}, \end{aligned} \quad (13)$$

one has

$$\lambda_{nl} = \frac{2\omega}{\pi^{1/2}} \frac{u_{nl}}{t_{nl} + v_{nl} - \omega}. \quad (14)$$

The identities (12) and (14) can be reconciled only if  $v_{nl} = \frac{1}{2}\omega$  for all  $n$  and  $l$ . Thanks to this  $(nl)$ -independence of  $v_{nl}$ , one has

$$\begin{aligned} &\left\langle \Psi_\infty(\omega; \mathbf{r}_1, \mathbf{r}_2) \left| \frac{1}{2}\omega^2(r_1^2 + r_2^2) \right| \Psi_\infty(\omega; \mathbf{r}_1, \mathbf{r}_2) \right\rangle \\ &= 2 \sum_{\mathbf{n}=1}^{\infty} \nu_{\mathbf{n}} v_{\mathbf{n}} = \omega \sum_{\mathbf{n}=1}^{\infty} \nu_{\mathbf{n}} = \omega, \end{aligned} \quad (15)$$

as expected.

The large- $n$  asymptotic estimates of  $t_{nl}$ ,  $v_{nl}$ , and  $u_{nl}$  are available from the general formalism previ-

ously applied to systems with Coulombic two-particle interactions.<sup>21</sup> They read

$$\tilde{t}_{nl} = \frac{\pi^2}{2} \frac{I_3}{I_1^3} n^2 = \frac{\pi}{3^{1/2}} \omega n^2, \quad (16)$$

$$\tilde{v}_{nl} = \frac{1}{I_1} \int_0^\infty \left( \frac{1}{2}\omega^2 r^2 \right) \exp\left(-\frac{1}{2}\omega r^2\right) dr = \frac{1}{2}\omega, \quad (17)$$

and

$$\tilde{u}_{nl} = \frac{I_3}{I_1} = 3^{-1/2}, \quad (18)$$

respectively, where  $I_\gamma = \int_0^\infty \exp(-4\omega r^2)^{\gamma/8} dr = \left(\frac{\pi}{2\gamma\omega}\right)^{1/2}$ .

The estimate of  $v_{nl}$  turns out to be exact, whereas those for  $t_{nl}$  and  $u_{nl}$  are consistent with the identities (9), (12), and (14). The same formalism yields

$$\tilde{\psi}_{nlm}(\omega; \mathbf{r}) = \left(\frac{8\omega}{\pi}\right)^{1/4} J_{l+\frac{3}{2}}(\chi_{nl})^{-1} \frac{\exp(-\frac{1}{4}\omega r^2)}{r} \operatorname{erf}\left((\omega/2)^{1/2} r\right)^{1/2} J_{l+\frac{1}{2}}\left(\chi_{nl} \operatorname{erf}\left((\omega/2)^{1/2} r\right)\right) Y_{lm}(\theta, \varphi) \quad (19)$$

for the large- $n$  asymptotic estimates  $\{\tilde{\psi}_{nlm}(\omega; \mathbf{r})\}$  of the NOs. In Eq. (19),  $J_l(t)$  is the  $l$ th Bessel function of the first kind and  $\chi_{nl}$  is the  $n$ th zero of  $J_{l+\frac{1}{2}}(t)$ .

## B. The 1-matrix and the collective occupancies

Let  $\Gamma(\omega; \mathbf{r}_{1'}, \mathbf{r}_1)$  be the 1-matrix (per spin) corresponding to  $\Psi(\omega; \mathbf{r}_1, \mathbf{r}_2)$ . As  $\omega \rightarrow \infty$ ,

$$\Gamma(\omega; \mathbf{r}_{1'}, \mathbf{r}_1) \rightarrow \Gamma_\infty(\omega; \mathbf{r}_{1'}, \mathbf{r}_1) = \frac{\omega^2}{\pi^3} \exp\left(-\frac{1}{2}\omega(r_1^2 + r_{1'}^2)\right) \int \frac{\exp(-\omega r_2^2)}{|\mathbf{r}_1 - \mathbf{r}_2| |\mathbf{r}_{1'} - \mathbf{r}_2|} d^3 \mathbf{r}_2, \quad (20)$$

where  $r_{1'} = |\mathbf{r}_{1'}|$ ; note the absence of the contributions arising from the  $-4\pi$  constant term in the definition of  $\Psi_\infty(\omega; \mathbf{r}_1, \mathbf{r}_2)$ . Upon insertion of the identity  $\frac{1}{|\mathbf{r}_1 - \mathbf{r}_2| |\mathbf{r}_{1'} - \mathbf{r}_2|} = \frac{1}{\pi} \int_{-\infty}^{\infty} \int_{-\infty}^{\infty} \exp[-\xi^2(\mathbf{r}_1 - \mathbf{r}_2)^2 - \xi'^2(\mathbf{r}_{1'} - \mathbf{r}_2)^2] d\xi d\xi'$ , followed by integration over  $\mathbf{r}_2$ , the change of variables  $\xi = \zeta^{-1}[\omega(1 - \zeta^2)]^{1/2} \cos \phi$  and  $\xi' = \zeta^{-1}[\omega(1 - \zeta^2)]^{1/2} \sin \phi$ , and then integration over  $\zeta$ , Eq. (20) becomes

$$\begin{aligned} \Gamma_\infty(\omega; \mathbf{r}_{1'}, \mathbf{r}_1) &= \frac{2\omega}{\pi^2} \int_0^\pi F(R, r, \vartheta; \phi)^{-1} \exp\left(-\frac{1}{2}\omega(F(R, r, \vartheta; \phi)^2 - 2rR \cos \vartheta \cos \phi)\right) \\ &\quad \times \left( \Re \left[ \exp\left(-\frac{1}{2}i\omega F(R, r, \vartheta; \phi)r \sin \vartheta\right) \operatorname{erfi}\left(\frac{1}{2}\omega^{1/2}(F(R, r, \vartheta; \phi) + ir \sin \phi)\right) \right] \right. \\ &\quad \left. - \sin\left(\frac{1}{2}\omega F(R, r, \vartheta; \phi)r \sin \phi\right) \right) d\phi, \end{aligned} \quad (21)$$

where  $i = \sqrt{-1}$ ,  $\Re z$  is the real part of  $z$ ,  $R = \frac{1}{2}|\mathbf{r}_1 + \mathbf{r}_{1'}|$ ,  $r = |\mathbf{r}_1 - \mathbf{r}_{1'}|$ ,  $\cos \vartheta = (r_1^2 - r_{1'}^2)/(2Rr)$ ,  $F(R, r, \vartheta; \phi) = (4R^2 + 4rR \cos \vartheta \cos \phi + r^2 \cos^2 \phi)^{1/2}$ , and  $\operatorname{erfi}(z)$  is the ‘‘imaginary error function’’ defined as  $\operatorname{erfi}(z) = -i \operatorname{erf}(iz)$ . Although the integral that enters Eq. (21) cannot be evaluated in a closed form, it is suitable for both numerical calculations and analysis of the properties of  $\Gamma_\infty(\omega; \mathbf{r}_{1'}, \mathbf{r}_1)$ . In particular, it readily yields the small- $r$  expansion

$$\Gamma_\infty(\omega; \mathbf{r}_{1'}, \mathbf{r}_1) = \frac{1}{\pi} \omega \exp(-2\omega R^2) \frac{\operatorname{erfi}(\omega^{1/2}R)}{R} - \frac{2}{\pi^2} \omega^2 \exp(-2\omega R^2) r + \dots \quad (22)$$

that, as expected, features a term linear in  $r$  (i.e. the particle coalescence cusp). The presence of this cusp leads to asymptotic decays of the  $m$ -independent occupation numbers that are consistent with those given by Eqs. (9) and (11).

For each azimuthal quantum number  $l$ , the collective occupancy (per spin and  $m$ )  $\eta_l = \sum_{n=1}^{\infty} \nu_{nl}$  is proportional to the norm of the  $l$ -wave in the partial-wave decomposition of  $\Psi_\infty(\omega; \mathbf{r}_1, \mathbf{r}_2)$ .<sup>22,23</sup> These occupancies, which satisfy the sum rule  $\sum_{l=0}^{\infty} (2l+1)\eta_l = 1$ , are given by the expression

$$\eta_l = \frac{2(2l+1) \left[ \psi\left(\frac{2l+3}{4}\right) - \psi\left(\frac{2l+5}{4}\right) \right] + 4}{(2l+1)^2 \pi}, \quad (23)$$

from which the large- $l$  behavior

$$\lim_{l \rightarrow \infty} \left(l + \frac{1}{2}\right)^3 \eta_l = \frac{1}{2\pi} \quad (24)$$

is readily deduced. The collective occupancy  $\eta_0 = 2-4/\pi \approx 0.726760$  of the  $s$ -type NOs indicates the persistence of strong correlation at  $\omega \rightarrow \infty$ . This limiting value is consistent with the general expression

$$\eta_0(\omega) = \frac{1}{1+\nu} + \frac{\left(\frac{\omega}{8\pi^3}\right)^{1/2} - 1}{(1+\nu)^2 \left[ \psi\left(-\nu - \frac{1}{2}\right) - \psi(-\nu) \right]} \quad (25)$$

valid for arbitrary  $\omega$ . Upon weakening of the confinement,  $\eta_0(\omega)$  decreases rapidly, as revealed by its values of  $\pi^2/(12 \ln 2) - \ln 2 \approx 0.493422$ ,  $(2\pi \ln 2 - 4)/(\pi(1 -$

$\ln 2)) \approx 0.368433$ , and  $(4 \ln 2 - 2)^{-1} - 1 \approx 0.294350$  computed with Eq. (24) at  $\omega$  equal to  $8\pi^3 \approx 248.050$ ,  $32\pi \approx 100.531$ , and  $2\pi^3 \approx 62.0126$ , respectively.

## C. Comparison with the strong-confinement limit of the two-electron harmonium atom

The normalized spatial component of the ground-state wave function of the two-electron harmonium atom described by the nonrelativistic Hamiltonian<sup>2-6</sup>

$$H = -\frac{1}{2}(\nabla_1^2 + \nabla_2^2) + \frac{1}{2}\omega^2(r_1^2 + r_2^2) + r_{12}^{-1} \quad (26)$$

is given by<sup>3,5</sup>

$$\begin{aligned} \Psi^\bullet(\omega; \mathbf{r}_1, \mathbf{r}_2) &= \left(\frac{\omega}{\pi}\right)^{3/2} \exp\left(-\frac{1}{2}\omega(r_1^2 + r_2^2)\right) \\ &\quad \times \left[ 1 + (2\omega)^{-1/2} \mathfrak{F}\left(\omega/2\right)^{1/2} r_{12} \right] \\ &\quad + \mathcal{O}(\omega^{-1}) \end{aligned} \quad (27)$$

at the limit of  $\omega \rightarrow \infty$ . The function

$$\begin{aligned} \mathfrak{F}(t) &= -2\pi^{-1/2}(1 + \ln 2) + t^{-1}[1 - \exp(t^2) \operatorname{erfc}(t)] \\ &\quad + 2 \int_0^t \exp(s^2) \operatorname{erfc}(s) ds \end{aligned} \quad (28)$$

that enters Eq. (27) has the small- $t$  expansion

$$\mathfrak{F}(t) = -2\pi^{-1/2} \ln 2 + t - \frac{2}{3}\pi^{-1/2}t^2 + \frac{1}{6}t^3 + \mathcal{O}(t^4), \quad (29)$$

which yields

$$\Psi_\infty^\bullet(\omega; \mathbf{r}_1, \mathbf{r}_2) = \left(\frac{\omega}{\pi}\right)^{3/2} \exp\left(-\frac{1}{2}\omega(r_1^2 + r_2^2)\right) \left(1 + \frac{1}{2}r_{12}\right) \quad (30)$$

as an analog of  $\Psi_\infty(\omega; \mathbf{r}_1, \mathbf{r}_2)$ .

By virtue of the aforementioned general formalism,<sup>21</sup> it follows from Eq. (30) that the asymptotic estimates analogous to  $\tilde{\lambda}_{nl}$ ,  $\tilde{\lambda}_n$ , and  $\tilde{v}_{nl}$  read<sup>24</sup>

$$\tilde{\lambda}_{nl}^\bullet = -\frac{4}{\pi^{5/2}} \omega^{-1/2} n^{-4}, \quad (31)$$

$$\tilde{\lambda}_n^\bullet = -\frac{2^{14/3}}{3^{10/3}\pi^{7/6}} \omega^{-1/2} n^{-4/3}, \quad (32)$$

$$\tilde{t}_{nl}^\bullet = \frac{\pi/2}{3^{1/2}} \omega n^2, \quad (33)$$

and

$$\tilde{v}_{nl}^\bullet = \omega, \quad (34)$$

respectively. The large- $n$  asymptotic estimate  $\tilde{u}_{nl}^\bullet$  of the  $m$ -independent expectation value  $u_{nl}^\bullet = \langle \psi_{nlm}^\bullet(\omega; \mathbf{r}) | \exp(-\frac{1}{2}\omega r^2) | \psi_{nlm}^\bullet(\omega; \mathbf{r}) \rangle$  that enters the analog

$$\tilde{\lambda}_{nl}^\bullet = -\frac{\omega^{3/2}}{\pi^{1/2}} \left( \frac{\tilde{u}_{nl}^\bullet}{\tilde{t}_{nl}^\bullet - \frac{1}{4}\tilde{v}_{nl}^\bullet} \right)^2 \quad (35)$$

of Eq. (12) equals  $3^{-1/2}$ , whereas those of  $\{\psi_{nlm}^\bullet(\omega; \mathbf{r})\}$  are given by<sup>21,24</sup>

$$\begin{aligned} \tilde{\psi}_{nlm}^\bullet(\omega; \mathbf{r}) &= \left(\frac{4\omega}{\pi}\right)^{1/4} J_{l+\frac{3}{2}}(\chi_{nl})^{-1} \frac{\exp(-\frac{1}{8}\omega r^2)}{r} \\ &\quad \times \operatorname{erf}(\omega^{1/2}r/2)^{1/2} \\ &\quad \times J_{l+\frac{1}{2}}(\chi_{nl} \operatorname{erf}(\omega^{1/2}r/2)) Y_{lm}(\theta, \varphi). \end{aligned} \quad (36)$$

Comparing Eqs. (19) and (36) reveals that  $\tilde{\psi}_{nlm}^\bullet(\omega; \mathbf{r}) = 2^{3/4} \tilde{\psi}_{nlm}^\bullet(\omega; 2^{1/2}\mathbf{r})$  for all the  $n$ ,  $l$ , and  $m$ . The identities  $\tilde{t}_{nl} = 2\tilde{t}_{nl}^\bullet$ ,  $\tilde{v}_{nl} = \frac{1}{2}\tilde{v}_{nl}^\bullet$ , and  $u_{nl} = u_{nl}^\bullet$  trivially follow from this relationship.

The collective occupancy (per spin and  $m$ )  $\eta_l^\bullet = \sum_{n=1}^{\infty} \nu_{nl}^\bullet$ , where  $\{\nu_{nl}^\bullet\} \equiv \{(\lambda_{nl}^\bullet)^2\}$  is readily obtained from the second-order perturbation theory,<sup>5,23</sup> which produces  $\eta_0^\bullet = 1 - (5 - 2\pi + 2 \ln 2)/(2\pi)\omega^{-1}$  and the ex-

pression

$$\begin{aligned} \eta_l^\bullet &= \frac{4^{-l}}{2\pi l^2(2l+1)^2} \left[ (2l+1) {}_3F_2 \left( \begin{matrix} l, l, l + \frac{1}{2} \\ l+1, 2l+2 \end{matrix} \middle| 1 \right) \right. \\ &\quad \left. - 2l {}_3F_2 \left( \begin{matrix} l, l + \frac{1}{2}, l + \frac{1}{2} \\ l + \frac{3}{2}, 2l+2 \end{matrix} \middle| 1 \right) \right] \omega^{-1} \end{aligned} \quad (37)$$

valid for  $l \neq 0$  that involves the hypergeometric functions. These occupancies exhibit the large- $l$  asymptotic behavior of  $\lim_{l \rightarrow \infty} (l + \frac{1}{2})^7 \eta_l^\bullet = 15/(32\pi)\omega^{-1}$ .

### III. NUMERICAL ANALYSIS

It is instructive to juxtapose the predictions presented in section II A against the results of numerical calculations. Of particular interest is the data computed for  $l = 0$  that pertains to the  $s$ -type NOs. Highly accurate approximations of these NOs are provided by the linear combinations

$$\psi_{n00}(\omega; \mathbf{r}) \approx \sum_{p=0}^{\mathfrak{N}} D_{n0,p}^{(\mathfrak{N})} f_{p00}(\omega; r) \quad (38)$$

of the square-normalized, i.e.  $\int_0^\infty |f_{p00}(\omega; r)|^2 4\pi r^2 dr = 1$  for all  $p$ , basis functions

$$\begin{aligned} f_{p00}(\omega; r) &= \left(\frac{\omega}{\pi}\right)^{3/4} \left[ \frac{(2p)!!}{(2p+1)!!} \right]^{1/2} L_p^{1/2}(\omega r^2) \\ &\quad \times \exp\left(-\frac{1}{2}\omega r^2\right) \end{aligned} \quad (39)$$

that are the eigenfunctions of the core Hamiltonian  $-\frac{1}{2}\nabla^2 + \frac{1}{2}\omega^2 r^2$  and involve the generalized Laguerre polynomials. The linear expansion coefficients  $\{D_{n0,p}^{(\mathfrak{N})}\}$  are the eigenvectors of the matrix  $\mathbf{G}^{(\mathfrak{N})}$  with the elements<sup>24</sup>

$$G_{pq}^{(\mathfrak{N})} = \left(\frac{2}{\pi}\right)^{1/2} 2^{-(p+q)} \frac{(2p+2q-1)!!}{[(2p+1)!(2q+1)!]^{1/2}}, \quad (40)$$

whereas the natural amplitudes  $\{\lambda_{n0}\}$  are approximated by the corresponding eigenvalues. For large  $p$ ,  $G_{pp}^{(\mathfrak{N})} \sim (2\pi)^{-1} p^{-3/2}$ .

The computation of the quantities pertaining to the  $\omega \rightarrow \infty$  limit of the two-electron harmonium atom involves analogous steps. For  $n \neq 1$ ,

$$\psi_{n00}^\bullet(\omega; \mathbf{r}) \approx \sum_{p=1}^{\mathfrak{N}} D_{n0,p}^{\bullet(\mathfrak{N})} f_{p00}(\omega; r), \quad (41)$$

where the linear expansion coefficients  $\{D_{n0,p}^{\bullet(\mathfrak{N})}\}$  are the eigenvectors of the matrix  $\mathbf{G}^{\bullet(\mathfrak{N})}$  with the elements

$$G_{pq}^{\bullet(\mathfrak{N})} = -\frac{(2/\pi)^{1/2} 4^{-(p+q)} (2p+2q-1)!}{[(2p+1)!(2q+1)!]^{1/2} (p+q)!} \omega^{-1/2} \quad (42)$$

Table I. The properties of the twenty  $s$ -type NOs with the largest occupation numbers.<sup>a</sup>

$n$	$\lambda_{n0}$	$\omega^{-1} v_{n0}$	$\omega^{-1} t_{n0}$	$u_{n0}$
1	$8.408176 \cdot 10^{-1}$	0.500000	5.526343	0.564894
3	$4.951911 \cdot 10^{-2}$	0.500000	13.563889	0.573311
4	$2.625255 \cdot 10^{-2}$	0.500000	25.239319	0.575578
5	$1.624173 \cdot 10^{-2}$	0.500000	40.548811	0.576457
6	$1.103445 \cdot 10^{-2}$	0.500000	59.490505	0.576870
7	$7.983664 \cdot 10^{-3}$	0.500000	82.063317	0.577088
8	$6.043756 \cdot 10^{-3}$	0.500000	108.266547	0.577213
9	$4.734019 \cdot 10^{-3}$	0.500000	138.099709	0.577288
10	$3.808275 \cdot 10^{-3}$	0.500000	171.562448	0.577335
11	$3.129825 \cdot 10^{-3}$	0.500000	208.654495	0.577365
12	$2.617812 \cdot 10^{-3}$	0.500000	249.375639	0.577385
13	$2.221921 \cdot 10^{-3}$	0.500000	293.725713	0.577398
14	$1.909512 \cdot 10^{-3}$	0.500000	341.704579	0.577407
15	$1.658657 \cdot 10^{-3}$	0.500000	393.312122	0.577413
16	$1.454183 \cdot 10^{-3}$	0.500000	448.548248	0.577416
17	$1.285323 \cdot 10^{-3}$	0.500000	507.412875	0.577418
18	$1.144259 \cdot 10^{-3}$	0.500000	569.905931	0.577419
19	$1.025208 \cdot 10^{-3}$	0.500000	636.027357	0.577419
20	$9.238179 \cdot 10^{-4}$	0.500000	705.777098	0.577419

<sup>a</sup> The approximate values computed for  $\mathfrak{N} = 2000$ .

and the natural amplitudes  $\{\lambda_{n0}^\bullet\}$  are approximated by the corresponding eigenvalues.<sup>25,26</sup> For large  $p$ ,  $G_{pp}^{\bullet(\mathfrak{N})} \sim -(8\pi)^{-1}\omega^{-1/2}p^{-5/2}$ .

Although the basis functions (38) give rise to readily evaluable matrix elements (39) and (41), the convergence of the computed data with the basis set size  $\mathfrak{N}$  is slow due to the smallness of the exponents ( $\frac{3}{2}$  and  $\frac{5}{2}$ , respectively) in the aforementioned power laws governing the decays of  $G_{pp}^{(\mathfrak{N})}$  and  $G_{pp}^{\bullet(\mathfrak{N})}$  with  $p$ . Consequently, expansions involving several thousands of these basis functions are required to produce reasonably accurate properties for tens of the NOs with the largest occupation numbers. A proper control of the concomitant roundoff errors requires the employment of arbitrary-precision arithmetic software.<sup>27</sup>

In Table I, the highly accurate values of  $\{\lambda_{n0}\}$ ,  $\{\omega^{-1} v_{n0}\}$ ,  $\{\omega^{-1} t_{n0}\}$ , and  $\{u_{n0}\}$  for  $1 \leq n \leq 20$  are compiled, whereas the corresponding  $\{\lambda_{n0}/\tilde{\lambda}_{n0}\}$ ,  $\{v_{n0}/\tilde{v}_{n0}\}$ ,  $\{t_{n0}/\tilde{t}_{n0}\}$ , and  $\{u_{n0}/\tilde{u}_{n0}\}$  ratios are displayed in Figs. 1–4 together with their counterparts for the two-electron harmonium atom at the  $\omega \rightarrow \infty$  limit. Inspection of these figures confirms the constancy of  $v_{n0}$  with respect to  $n$  and the rapid rates at which  $\lambda_{n0}$ ,  $t_{n0}$ ,  $u_{n0}$ ,  $\lambda_{n0}^\bullet$ ,  $v_{n0}^\bullet$ ,  $t_{n0}^\bullet$ , and  $u_{n0}^\bullet$  approach their respective large- $n$  asymptotics.

The plots of the scaled NOs presented for  $n = 1$  [note that  $\psi_{100}^\bullet(\omega; \mathbf{r}) = f_{000}(\omega; r)$ ] and  $n = 2$  in Figs. 5a and 5b are quite similar. At larger  $n$  (Figs. 5c and 5d), they become virtually indistinguishable, demonstrating

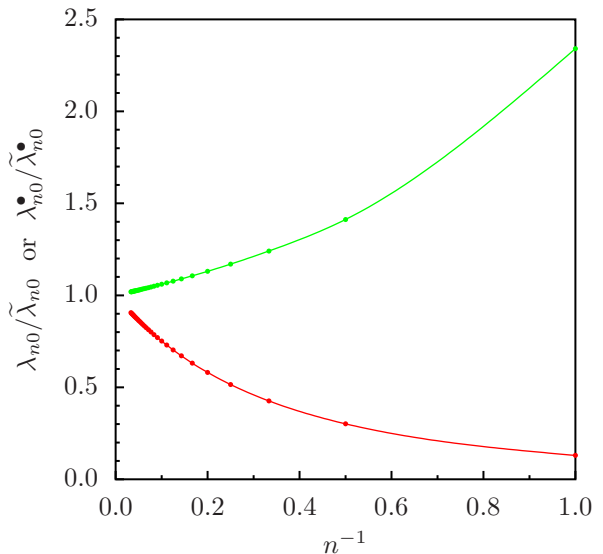


Figure 1. The  $\lambda_{n0}/\tilde{\lambda}_{n0}$  (green) and  $\lambda_{n0}^\bullet/\tilde{\lambda}_{n0}^\bullet$  (red) ratios vs.  $n^{-1}$  for  $1 \leq n \leq 30$ . The lines are provided for eye guidance only.

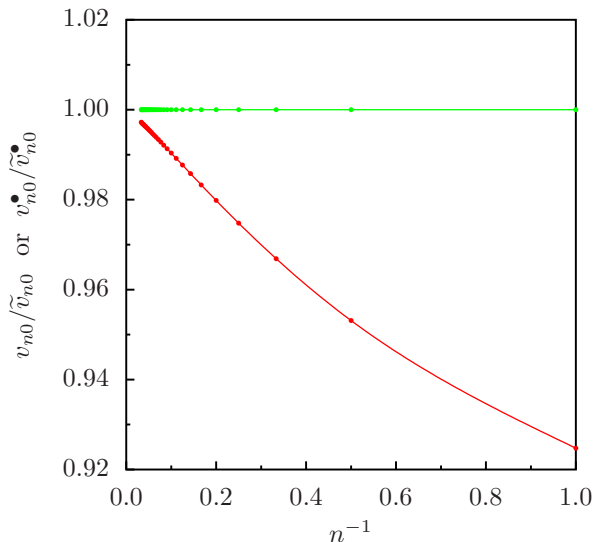


Figure 2. The  $v_{n0}/\tilde{v}_{n0}$  (green) and  $v_{n0}^\bullet/\tilde{v}_{n0}^\bullet$  (red) ratios vs.  $n^{-1}$  for  $1 \leq n \leq 30$ . The lines are provided for eye guidance only.

the remarkable accuracy of the approximate identity  $\psi_{n00}(\omega; \mathbf{r}) \approx 2^{3/4}\psi_{n00}^\bullet(\omega; 2^{1/2}\mathbf{r})$  that follows from the asymptotic estimates (19) and (36). Although, strictly speaking, these estimates are valid only at the  $n \rightarrow \infty$  limit, the approximate identity appears to be closely followed already for  $n = 11$ .

#### IV. DISCUSSION AND CONCLUSIONS

There are many peculiarities inherent in the one-particle description of the contactium. Some of them

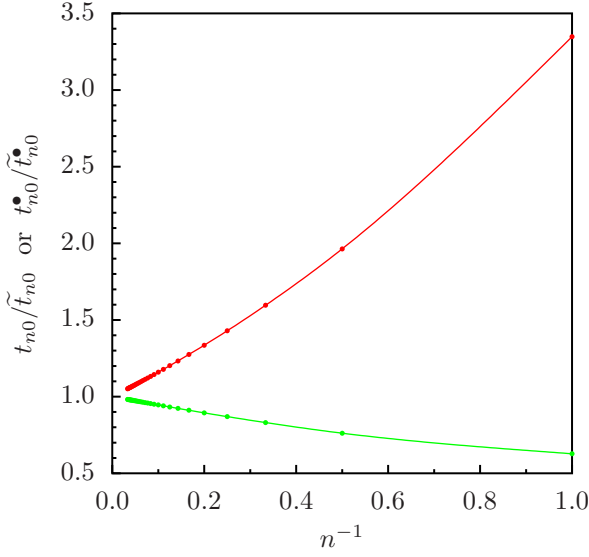


Figure 3. The  $t_{n0}/\tilde{t}_{n0}$  (green) and  $t_{n0}^\bullet/\tilde{t}_{n0}^\bullet$  (red) ratios vs.  $n^{-1}$  for  $1 \leq n \leq 30$ . The lines are provided for eye guidance only.

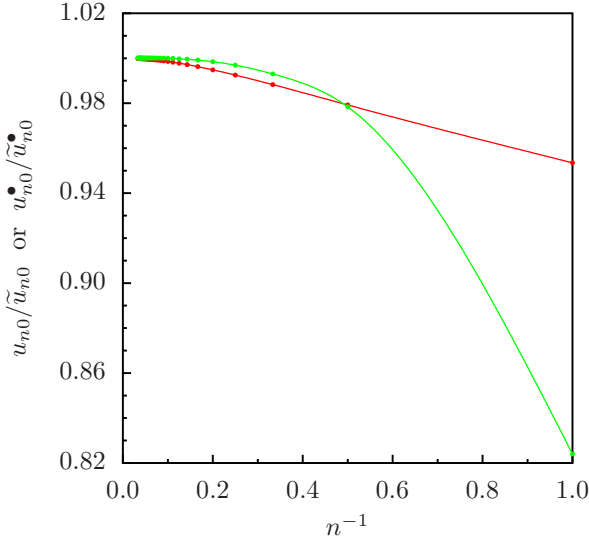


Figure 4. The  $u_{n0}/\tilde{u}_{n0}$  (green) and  $u_{n0}^\bullet/\tilde{u}_{n0}^\bullet$  (red) ratios vs.  $n^{-1}$  for  $1 \leq n \leq 30$ . The lines are provided for eye guidance only.

follow directly from the infinite values of the kinetic and interparticle interaction energies. Thus, combining Eqs. (11), (12), (14), and (18) yields the asymptotic power law

$$\lim_{n \rightarrow \infty} n^{2/3} \nu_n t_n = \lim_{n \rightarrow \infty} \frac{2\omega}{(3\pi)^{1/2}} n^{2/3} \lambda_n = \frac{2^{10/3}}{3^{13/6} \pi^{4/3}} \omega \quad (43)$$

for the contribution  $\nu_n t_n$  of the  $n$ th NO to the kinetic energy. Consequently, the sum  $\sum_{n=1}^{\infty} \nu_n t_n$  diverges, as expected. On the other hand, the kinetic energy  $T_{KS}$  of the fictitious noninteracting system involved in the description of the contactium within the Kohn–Sham

formalism<sup>28</sup> is finite, i.e.

$$T_{KS} = \frac{1}{2} \int |\nabla \sqrt{\rho_\infty(\omega; \mathbf{r})}|^2 d^3 \mathbf{r} \approx 1.130576 \omega \quad (44)$$

where [compare with Eq. (22)]

$$\rho_\infty(\omega; \mathbf{r}) = \frac{1}{\pi} \omega \exp(-2\omega r^2) \frac{\operatorname{erfi}(\omega^{1/2} r)}{r} \quad (45)$$

is the one-particle density (per spin).

In analogy to that of a Coulombic system, the interparticle interaction energy of the contactium can be formally partitioned into the direct, exchange, and correlation contributions. For the first two of those, one obtains

$$\begin{aligned} J &= 2 \iint \rho_\infty(\omega; \mathbf{r}_1) \rho_\infty(\omega; \mathbf{r}_2) \delta_{\text{reg}}(\mathbf{r}_{12}) d^3 \mathbf{r}_1 d^3 \mathbf{r}_2 \\ &= 2 \int \rho_\infty(\omega; \mathbf{r})^2 d^3 \mathbf{r} = \frac{4}{\pi^{3/2}} \arctan(2^{-3/2}) \omega^{3/2} \end{aligned} \quad (46)$$

and

$$\begin{aligned} K &= - \iint |\Gamma_\infty(\omega; \mathbf{r}_1, \mathbf{r}_2)|^2 \delta_{\text{reg}}(\mathbf{r}_{12}) d^3 \mathbf{r}_1 d^3 \mathbf{r}_2 \\ &= - \int \rho_\infty(\omega; \mathbf{r})^2 d^3 \mathbf{r} = - \frac{2}{\pi^{3/2}} \arctan(2^{-3/2}) \omega^{3/2}, \end{aligned} \quad (47)$$

respectively. Although these contributions are finite-valued, they scale like  $\omega^{3/2}$  rather than  $\omega$ , as would be expected from the overall scaling of the energy. The correlation contribution is both negative and infinite.

For Coulombic systems, the 1-RDMFT formalism involves only a single component (i.e. the correlation part of the electron–electron repulsion energy) of the total energy that is given by an unknown functional. In contrast, there are three energy components (i.e. the kinetic energy together with the exchange and correlation part of the electron–electron repulsion energy) within DFT for which one has to resort to approximate expressions. In the case of the contactium, this advantage enjoyed by 1-RDMFT over DFT is lost as the kinetic and interparticle interaction contributions to the total energy can no longer be considered separately. On the other hand, taking into account the aforementioned finite-valuedness of  $T_{KS}$ , one expects a reasonable description of many-particle analogs of the contactium with the Kohn–Sham approach, provided a suitable functional is constructed.

The present study leads to the somewhat surprising conclusion that almost identical natural orbitals can pertain to two systems with diametrically different interparticle interactions giving rise to entirely different behavior of the respective wave functions at the spatial two-particle coalescences. It thus appears that the gross of the information about these interactions is contained in the occupation numbers or, to be more precise, in their asymptotic dependence on the ordinal number. This observation strongly suggests that quantitative measures

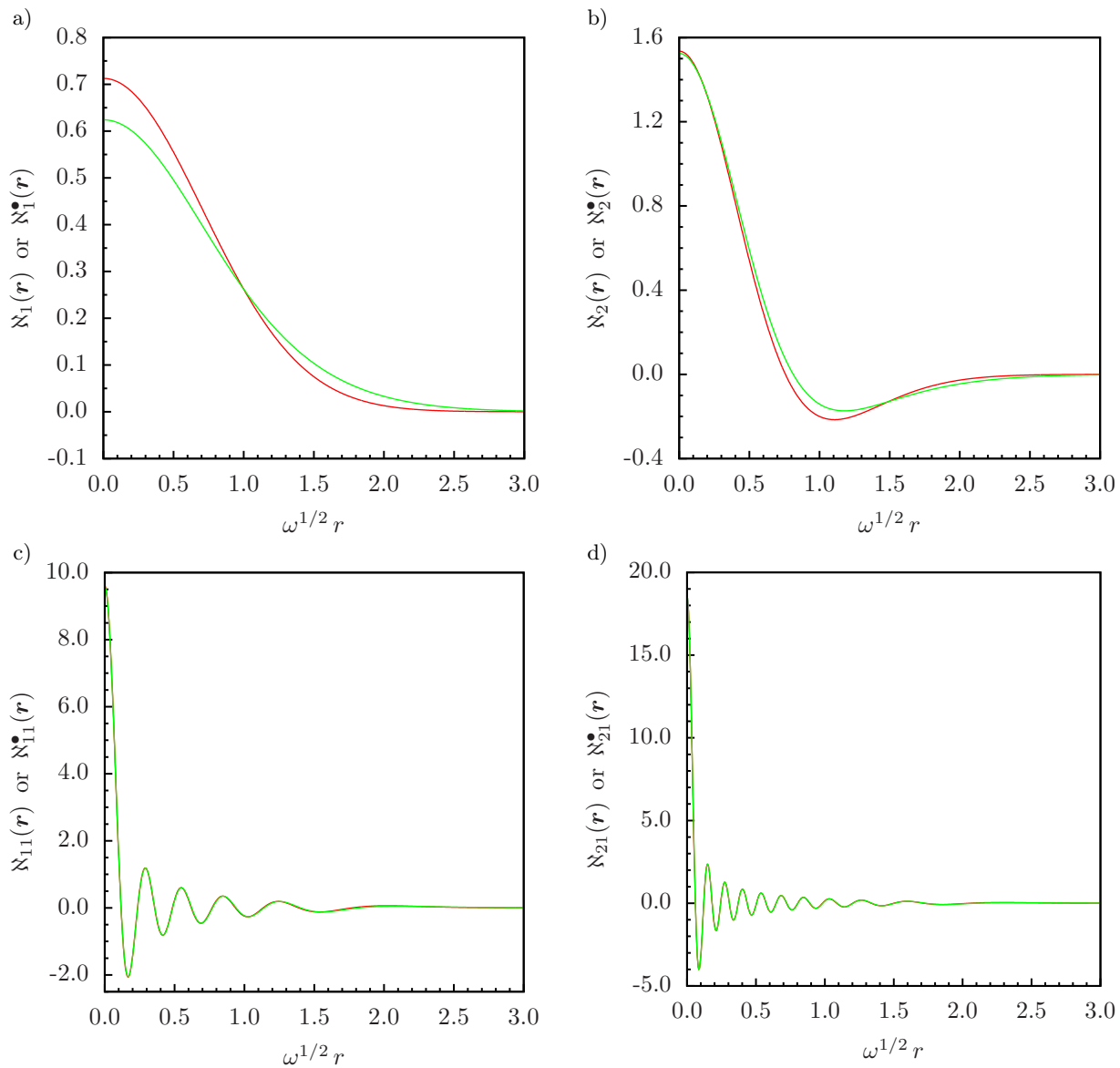


Figure 5. The scaled NOs  $\aleph_n(r) \equiv \omega^{-3/4}\psi_{n00}(\omega; \mathbf{r})$  (green) and  $\aleph_n^\bullet(r) \equiv (\omega/2)^{-3/4}\psi_{n00}^\bullet(\omega; 2^{1/2}\mathbf{r})$  (red) vs.  $\omega^{1/2}r$  for a)  $n = 1$ , b)  $n = 2$ , c)  $n = 11$ , and d)  $n = 21$ .

of particle correlation based upon one-particle quantities should be constructed from the occupation numbers rather than properties of the corresponding natural orbitals.

The unusual properties of contactium are bound to stimulate further research on strongly correlated systems. Of particular interest is the extension of the present study to species involving large numbers of either fermions or bosons subject to various confining potentials.

#### ACKNOWLEDGMENTS

The research described in this publication has been funded by the National Science Center (Poland) under

grant 2018/31/B/ST4/00295 and supported by the National Research Foundation, Singapore and A\*STAR under its CQT Bridging Grant and its Quantum Engineering Programme (grant NRF2022-QEP2-02-P16 supports J.H.H.). One of the authors (J.C.) thanks the good people of CQT for their splendid hospitality during his stay in Singapore.

#### REFERENCES

- <sup>1</sup>T. Helgaker, P. Jørgensen, J. Olsen, *Molecular Electronic-Structure Theory* (John Wiley & Sons, Chichester, 2000).
- <sup>2</sup>M. Taut, *Phys. Rev. A* **48**, 3561 (1993); *J. Phys. A* **27**, 1045 (1994); **27**, 4723(E) (1994).
- <sup>3</sup>J. Cioslowski and K. Pernal, *J. Chem. Phys.* **113**, 8434 (2000).



- <sup>4</sup>H. F. King, *Theor. Chim. Acta* **94**, 345 (1996).
- <sup>5</sup>R. J. White and W. Byers Brown, *J. Chem. Phys.* **53**, 3869 (1970).
- <sup>6</sup>N. R. Kestner and O. Sinanoğlu, *Phys. Rev.* **128**, 2687 (1962).  
E. Santos, *Anal. R. Soc. Esp. Fis. Quim.* **64**, 177 (1968).
- <sup>7</sup>C. Filippi, C. J. Umrigar, and M. Taut, *J. Chem. Phys.* **100**, 1290 (1994).  
S. Ivanov, K. Burke, and M. Levy, *ibid.* **110**, 10262 (1999).  
M. Taut, A. Ernst, and H. Eschrig, *J. Phys. B* **31**, 2689 (1998).  
P. Gori-Giorgi and A. Savin, *Int. J. Quantum Chem.* **109**, 2410 (2009).
- <sup>8</sup>M. Rodríguez-Mayorga, E. Ramos-Cordoba, M. Via-Nadal, M. Piris, and E. Matito, *Phys. Chem. Chem. Phys.* **19**, 24029 (2017).  
K. J. H. Giesbertz and R. van Leeuwen, *J. Chem. Phys.* **139**, 104110 (2013).  
S. Crisostomo, M. Levy, and K. Burke, *J. Chem. Phys.* **157**, 154106 (2022).  
D. P. Kooi and P. Gori-Giorgi, *Theor. Chem. Acc.* **137**, 166 (2018).  
S. Śmiga, F. D. Sala, P. Gori-Giorgi, and E. Fabiano, *J. Chem. Theory Comput.* **18**, 5936 (2022).
- <sup>9</sup>P.-F. Loos and P. M. W. Gill, *Phys. Rev. Lett.* **103**, 123008 (2009).
- <sup>10</sup>P.-F. Loos and P. M. W. Gill, *J. Chem. Phys.* **132**, 234111 (2010).  
J. Jung and J. E. Alvarillos, *J. Chem. Phys.* **118**, 10825 (2003).  
D.C. Thompson and A. Alavi, *Phys. Rev. B* **66**, 235118 (2002); **68**, 039901(E) (2003).
- <sup>11</sup>For a recent review see: K. Pernal and K. J. H. Giesbertz, *Top. Curr. Chem.* **368**, 125 (2016).
- <sup>12</sup>C. L. Benavides-Riveros, J. Wolff, M. A. L. Marques, and C. Schilling, *Phys. Rev. Lett.* **124**, 180603 (2020).
- <sup>13</sup>J. Cioslowski, *J. Chem. Theory Comput.* **16**, 1578 (2020).
- <sup>14</sup>E. Fermi, *Ricerca Scient.* **7**, 13 (1936).
- <sup>15</sup>K. Huang and C. N. Yang, *Phys. Rev.* **105**, 767 (1957).
- <sup>16</sup>For a review, see for example: D. Blume, *Rep. Prog. Phys.* **75**, 046401 (2012).
- <sup>17</sup>T. Busch, B.-G. Englert, K. Rzażewski, and M. Wilkens, *Found. Phys.* **28**, 549 (1998).
- <sup>18</sup>P.-O. Löwdin and H. Shull, *Phys. Rev.* **101**, 1730 (1956).
- <sup>19</sup>K. Chadan, *Il Nuovo Cimento A*, **58**, 191 (1968).
- <sup>20</sup>A. Martin, *Helv. Phys. Acta* **45**, 140 (1972); H. Tamura, *Proc. Japan Acad.* **50**, 19 (1974).
- <sup>21</sup>J. Cioslowski and K. Strasburger, *J. Chem. Theory Comput.* **17**, 6918 (2021).
- <sup>22</sup>J. Cioslowski and F. Prątnicki, *J. Chem. Phys.* **150**, 074111 (2019).
- <sup>23</sup>J. Cioslowski, *Theor. Chem. Acc.* **134**, 113 (2015).
- <sup>24</sup>J. Cioslowski, *J. Chem. Phys.* **148**, 134120 (2018).
- <sup>25</sup>J. Cioslowski, *Theor. Chem. Acc.* **137**, 173 (2018).
- <sup>26</sup>J. Cioslowski and F. Prątnicki, *J. Chem. Phys.* **151**, 184107 (2019).
- <sup>27</sup>Mathematica, Version 12.2.0.0, Wolfram Research, Inc., Champaign, IL, 2020.
- <sup>28</sup>W. Kohn, and L. J. Sham, *Phys. Rev.*, A1133 (1965).